Small Molecule Therapeutics

Molecular Cancer Therapeutics

Targeting TAO Kinases Using a New Inhibitor Compound Delays Mitosis and Induces Mitotic Cell Death in Centrosome Amplified Breast Cancer Cells

Chuay-Yeng Koo[1], Caterina Giacomini[1], Marta Reyes-Corral[1], Yolanda Olmos[1], Ignatius A. Tavares[1], Charles M. Marson[2], Spiros Linardopoulos[3], Andrew N. Tutt[3,4], and Jonathan D.H. Morris[1]

Abstract

Thousand-and-one amino acid kinases (TAOK) 1 and 2 are activated catalytically during mitosis and can contribute to mitotic cell rounding and spindle positioning. Here, we characterize a compound that inhibits TAOK1 and TAOK2 activity with IC_{50} values of 11 to 15 nmol/L, is ATP-competitive, and targets these kinases selectively. TAOK inhibition or depletion in centrosome-amplified SKBR3 or BT549 breast cancer cell models increases the mitotic population, the percentages of mitotic cells displaying amplified centrosomes and multipolar spindles, induces cell death, and inhibits cell growth. In contrast, nontumorigenic and dividing bipolar MCF-10A breast cells appear less dependent on TAOK activity and can complete mitosis and proliferate in the presence of the TAOK inhibitor. We demonstrate that TAOK1 and TAOK2 localize to the cytoplasm and centrosomes respectively during mitosis. Live cell imaging shows that the TAOK inhibitor prolongs the duration of mitosis in SKBR3 cells, increases mitotic cell death, and reduces the percentages of cells exiting mitosis, whereas MCF-10A cells continue to divide and proliferate. Over 80% of breast cancer tissues display supernumerary centrosomes, and tumor cells frequently cluster extra centrosomes to avoid multipolar mitoses and associated cell death. Consequently, drugs that stimulate centrosome declustering and induce multipolarity are likely to target dividing centrosome-amplified cancer cells preferentially, while sparing normal bipolar cells. Our results demonstrate that TAOK inhibition can enhance centrosome declustering and mitotic catastrophe in cancer cells, and these proteins may therefore offer novel therapeutic targets suitable for drug inhibition and the potential treatment of breast cancers, where supernumerary centrosomes occur. *Mol Cancer Ther; 1–12.* ©2017 AACR.

Introduction

Thousand-and-one amino acid kinases (TAOK, also referred to as PSKs) belong to the sterile 20 (STE20) group of kinases, and subfamily members include TAOK1, TAOK2, and TAOK3 (1–6). TAOKs can regulate MAPK signaling pathways, and TAOK1 or TAOK2, but not TAOK3, stimulate c-Jun N-terminal kinase (JNK) and p38 MAPKs (1–5). TAOK1 and TAOK2 also induce apoptotic morphologic changes via their activation of JNK MAPK and caspases (4, 5). Additional studies have shown that TAOKs can regulate microtubule (MT) dynamics and organization (7–9). TAOK1 induces MT instability via activation of MT-affinity–regulating kinase (MARK/PAR-1) and phosphorylation of the MT-associated protein tau, which dissociates from MTs, resulting in their disassembly (8–11). TAOK2 can bind to MTs via its C terminus (amino acids 745–1235) and produces stabilized perinuclear MT cables that are nocodazole-resistant (7). TAOKs appear to be activated during MT-dependent processes when increases in MT dynamics occur, and these events include mitosis and neuritogenesis (12, 13). Our recent work using small-interfering RNA (siRNA) to deplete TAOK1 or TAOK2 has shown that these proteins are required for mitotic cell rounding and spindle positioning, consistent with functional roles for these proteins in regulating MTs and mitosis (12).

Many cancer drugs are antiproliferative and disrupt MTs during cell division and include the original antimitotic drugs such as taxanes and vinca alkaloids (14, 15). Perturbation of the mitotic spindle results in erroneous chromosome alignment and activation of the spindle-assembly checkpoint, which prevents mitotic progression and results in cell death (16, 17). Mitotic catastrophe provides an onco-suppressive mechanism that is activated during or after defective mitosis and results in cell death or senescence that is distinct from apoptosis (18, 19). Cell death may occur during mitosis or after premature slippage out of mitosis, or alternatively, cells may become senescent in the subsequent G_1 phase of the cell cycle following mitotic slippage (18, 19). Mitotic catastrophe therefore provides a mechanism for avoiding

[1]King's College London, School of Cancer Sciences, New Hunt's House, Guy's Campus, Great Maze Pond, London, United Kingdom. [2]Department of Chemistry, Christopher Ingold Laboratories, University College London, London, United Kingdom. [3]Breast Cancer Now Toby Robins Research Centre, the Institute of Cancer Research, London, United Kingdom. [4]King's College London, School of Cancer Sciences, Breast Cancer Now Research Unit, Guy's Cancer Centre, Guy's Hospital, London, United Kingdom.

Note: Supplementary data for this article are available at Molecular Cancer Therapeutics Online (http://mct.aacrjournals.org/).

Corresponding Author: Jonathan D.H. Morris, King's College London, Guy's Campus, Great Maze Pond, London SE11UL, UK. Phone: 44-20-78488302; Fax: 44-20-78486620; E-mail: jonathan.morris@kcl.ac.uk

doi: 10.1158/1535-7163.MCT-17-0077

genomic instability; however, its induction may also provide a therapeutic opportunity whereby drugs and MT poisons disrupt the mitotic machinery and induce cancer cell death. Conventional MT-targeting drugs such as docetaxel, paclitaxel, and epothilones, have proven to be clinically effective and are relatively cancer specific, but these compounds are also prone to debilitating side effects, and patient relapse commonly occurs due to drug resistance (14, 20, 21). Consequently, current efforts are underway to develop a new generation of mitosis-selective drugs that are designed to inhibit proteins with essential roles in mitosis. Classic mitotic kinases such as the cyclin-dependent kinases, Polo-like kinases, and Aurora kinases have been targeted already and showed efficacy in recent clinical trials; however, these drugs also appear to have limited efficacy in solid tumors and can cause severe side effects (22–25).

Additional strategies are now required to target cancer-specific events that are essential for tumor cell survival. Many solid and hematologic cancers exhibit supernumerary centrosomes, and tumor cells often cluster extra centrosomes to produce a functional bipolar-like spindle. Drugs that induce declustering of centrosomes and stimulate multipolar mitosis and cell death could therefore target and kill cancer cells selectively. Here, we have characterized a small-molecule inhibitor of the TAOK family of protein kinases and shown that TAOK inhibition can increase centrosome declustering, delay mitotic progression, and induce mitotic catastrophe in centrosome-amplified SKBR3 breast cancer cells. In contrast, nontumorigenic and bipolar MCF-10A breast cells appear more resistant to the TAOK inhibitor and continue to divide in its presence.

Materials and Methods

Reagents and antibodies

PRK5-MYC vector, pRK5-MYC-TAOK1, pRK5-MYC-TAOK1 (K57A), pRK5-MYC-TAOK2, and pRK5-MYC-TAOK2 (K57A) were made as described previously (1, 5). PCMV-FLAG-JNK1 was a gift from Dr. M. Karin (University of California, USA). siRNA oligonucleotide sequences targeting TAOK1 (#1 and #4) or TAOK2 (#1 and #4) were described previously (12). Recombinant TAOK1 (1-319) and TAOK2 (1-319) were purchased from SignalChem (#T24-11G, #T25-11G). Rabbit TAOK1 or TAOK2 antibodies were obtained from Proteintech (#26250, #21188), and TAOK-pS181 antibody was produced by Eurogentec (4). Rabbit anti-FLAG and mouse anti–α-tubulin (DM1A) or anti-MYC antibodies and DAPI were obtained from Sigma-Aldrich (#F7425, #T9026, #M5546), and rabbit anti–JNK-pT183/Y185 antibody was purchased from Cell Signaling Technology (#9251). Mouse anti-GFP antibodies were obtained from Millipore (#MAB3850). Rabbit anti-pericentrin and anti–α-tubulin antibodies were purchased from AbCam (#ab44481, #ab18251). Goat anti-rabbit Alexa-Fluor568 and Goat anti-mouse Alexa-Fluor488 antibodies were obtained from ThermoFisher Scientific (#A11036, #A11029).

Cell culture and overexpression or knockdown of TAOKs

Cell lines were obtained from the ATCC (2008) and authenticated with karyotyping and short tandem repeat DNA profiling (2014). Cells were frozen within 4 weeks of purchase and used within 10 weeks after resuscitation and media checked routinely for mycoplasma using DAPI staining. MCF10-A cells were grown in DMEM/F12 Ham medium containing 5% horse serum (Sigma-Aldrich, #H1138), 20 ng/mL EGF (Sigma-Aldrich, #E4127), 100 ng/mL cholera toxin (Sigma-Aldrich, #C8052), 500 ng/mL hydrocortisone (Sigma-Aldrich, #H4001), and 10 μg/mL insulin (Sigma-Aldrich, #I9278). SKBR3 cells were maintained in McCoy's/5A medium supplemented with 10% FCS. COS1 cells were grown in DMEM supplemented with 10% FCS. BT549 cells were grown in RPMI containing 10 μg/mL insulin and 10% FCS (ThermoFisher #10270). All media contained antibiotics and cultures grown in a humidified atmosphere (10% CO_2, 37°C). For soft-agar growth and colony formation assays, cells were plated in growth medium and 0.3% SeaPlaque low-melting agarose (Lonza, #50101). The bottom layer was made up of growth medium and 0.6% agarose. Colonies were stained with 0.005% crystal violet. For transfection, cells were treated with the indicated plasmids and Lipofectamine 2000 according to the manufacturer's instructions (ThermoFisher Scientific, #1166027). For TAOK depletion experiments, growing cells were treated with the indicated siRNA (50 nmol/L) oligonucleotides targeting TAOKs and HiPerFect (Qiagen, #301705) as described previously, and cells on the culture plate and in the media pooled to determine cell numbers (12).

Immunoprecipitation and Western blot analysis

Transfected COS1 cells were incubated for 22 hours and then extracted in lysis buffer (500 μL; ref. 12). For immunoprecipitation, samples were mixed with 15 μL of mouse anti–FLAG-agarose beads (Sigma-Aldrich, #A2220) for 2 hours/4°C and then washed in lysis buffer (x4) and bead pellets extracted in gel sample buffer. Protein extracts were resolved by SDS-PAGE (10%) followed by immunoblotting with the indicated antibodies, and blot patterns were analyzed using ECL and densitometry (1).

Flow cytometry

Cells were treated with compound 43 (10 μmol/L or equivalent DMSO) for 24 to 72 hours. To determine the mitotic fraction, cells were fixed with 2% PFA/PBS for 10 minutes, permeabilized with 90% methanol, and blocked in 0.5% BSA/PBS before staining with Alexa-Fuor488-histoneH3-pS10 antibody (Cell Signaling Technology #3465, 1 hour). Cells were then washed twice and stained with propidium iodide (PI). To assess apoptosis, FITC–Annexin V antibody (ThermoFisher Scientific #A13201) was used. Cells were resuspended in Annexin-binding buffer and stained with 5 μL of FITC–Annexin V antibody and PI for 30 minutes. Fluorescence from both assays was measured using a FACS Canto II flow cytometer (BD Technologies).

Immunostaining, confocal, and time-lapse video microscopy

Growing cells on coverslips were fixed with ice-cold methanol (5 minutes/4°C) or 4% paraformaldehyde/PBS (15 minutes/RT). Alternatively, SKBR3 cells containing doxycycline-inducible pRetroX-TRE3G-GFP-TAOK plasmids were seeded on poly-L-lysine–coated coverslips and incubated with 10 ng/μL doxycycline (Sigma-Aldrich, #D9891) for 24 hours before fixation. Samples were costained with the indicated antibodies and DAPI (3 μmol/L) and processed as described previously (12), and cells imaged using a CSU-X1–inverted spinning-disk confocal microscope (Nikon) equipped with a EM-CCD camera (Andor iXon3) and a 100x/1.40 NA oil objective (Nikon). Z-stacks were taken using a 0.3 μm step size. For time-lapse video imaging and mitotic cell analysis, MCF-10A or SKBR3 cells expressing GFP-α-tubulin constitutively were seeded onto a 24-well plate (Ibidi) and incubated overnight. Cultures were treated with compound 43 or DMSO as

indicated and imaged at 15-minute intervals over a 48-hour period. Time-lapse imaging was carried out using an Eclipse Ti-E Inverted microscope (Nikon), equipped with a 20x air objective (Nikon), a cooled CCD camera (CoolSNAP HQ2, Photometrics), and a climate-controlled chamber (37°C/5% CO_2). The time of mitotic duration (nuclear envelope breakdown to cytokinesis) and mitotic catastrophe or exit from mitosis was determined by visual inspection and scoring of >120 individual cells per condition and for each experiment ($n = 3$).

TAOK inhibitor compounds

Compounds 43 and 63 were synthesized by Evotec Limited (UK) and characterized using KinaseProfiler services provided by Eurofins (Supplementary Methods).

Statistical analysis

Graphs and statistical analysis one-way or two-way ANOVA followed by a Bonferroni correction were performed using GraphPad, and results are presented as mean ± SD.

Results

Identification and synthesis of small-molecule inhibitors for TAO kinases

Our previous studies have used siRNA to demonstrate that TAOK1 and TAOK2 expression in HeLa cells is required for mitotic cell rounding and spindle positioning, and these results suggest that small-molecule TAOK inhibitors are likely to perturb malignant cell division (12). Currently, no effective TAOK inhibitors have been reported in the literature; however, Exelixis Inc. have patented several compounds that may inhibit TAOKs with IC_{50} values $\leq$ 50 nmol/L (WO2005/040355A2; ref. 26). Two of these compounds were synthesized for this study by Evotec and include *N*-[2-oxo-2-(1,2,3,4-tetrahydronaphthalen-1-ylamino)ethyl]biphenyl-4-carboxamide (referred to hereafter as compound 43 using Exelixis Inc. nomenclature) and *N*-{3-[(2-{[6-methoxy-1,3-benzothiazol-2-yl]amino}-2-oxoethyl)amino]-3-oxo-1-phenylpropyl}benzamide (referred to hereafter as compound 63; Fig. 1A).

Compounds 43 and 63 inhibit TAOK activity *in vitro*

Initial experiments were set out to confirm that both compounds could inhibit TAOK catalytic activity in *in vitro* kinase assays. Purified TAOKs were incubated with concentrations of compound 43 or 63 between 0 and 30 μmol/L; both compounds inhibit MBP phosphorylation by TAOK1 or TAOK2 potently (Fig. 1B). Calculated IC_{50} values for TAOK inhibition by compound 43 were 11 nmol/L for TAOK1 and 15 nmol/L for TAOK2 (Fig. 1B). Compound 63 also inhibited TAOK activity with IC_{50} values of 19 nmol/L for TAOK1 and 39 nmol/L for TAOK2 (Fig. 1B).

Compounds 43 and 63 inhibit TAOK activity selectively

The specificity of compound inhibition for TAOKs was examined by repeating *in vitro* kinase assays using 70 different kinases. TAOK1 or TAOK2 retained 8% and 11% of their activity, respectively, when incubated in the presence of compound 43 (0.3 μmol/L) and compared with control samples (Fig. 1C). Of the other kinases examined here, TAOK3 was inhibited and retained 13% activity. Three structurally related STE20 family members, LOK (48% activity retained), TAK1 (53% activity retained), and PAK2 (79% activity retained), were also inhibited by compound 43, *albeit* to a lesser extent than the TAOKs. In addition, EphB4 (61% activity retained) and Aurora-B (82% activity retained) are inhibited partially by this small molecule; however, the remaining 62 kinases tested here retained $\geq$ 80% of their activity in the presence of compound 43 (Fig. 1C and Supplementary Table S1). TAOK1 or TAOK2 also retained 11% of their activity, when incubated with compound 63 (0.3 μmol/L) and compared with control samples (Fig. 1C). Of the other kinases analyzed, TAOK3 was inhibited and retained 13% of activity, whereas ALK retained 64% activity, CDK9 retained 67% activity, SAPK2a and RSK1 retained 77% activity, and DRAK1 retained 70% activity, in the presence of compound 63 (Fig. 1C). Sixty-two other kinases retained $\geq$ 80% of their activity when incubated with compound 63 (Fig. 1C and Supplementary Table S1). Notably, the mitotic kinases Aurora A and B, Plk1 and 3, as well as CDK1 and 2 retain $\geq$80% of their catalytic activity with either compound (Fig. 1C). These results demonstrate that compounds 43 and 63 inhibit the catalytic activity of TAOKs selectively, when compared with their effects on alternative kinases.

Compounds 43 and 63 are ATP-competitive inhibitors of TAOK activity

ATP-competitive binding assays were carried out to investigate the mechanism of action for both TAOK inhibitors. *In vitro* kinase assays were repeated using nine concentrations of either compound 43 or 63 (between 0 and 1 μmol/L), ATP (1, 10, or 155 μmol/L), and purified TAOK1 or TAOK2. For compound 43, increasing [ATP] from 10 to 155 μmol/L raised the calculated IC_{50} values from 5 to 139 nmol/L for TAOK1, and from 7 to 137 nmol/L for TAOK2 (Supplementary Fig. S1A). For compound 63, increasing [ATP] from 10 to 155 μmol/L raised the calculated IC_{50} values from 20 to 170 nmol/L for TAOK1, and from 28 to 221 nmol/L for TAOK2 (Supplementary Fig. S1B). Both compounds are therefore ATP-competitive inhibitors of TAOK1 or TAOK2 activity.

Compound 43 inhibits TAOK stimulation of JNK in cells

Exogenous TAOK1 or TAOK2 can stimulate the phosphorylation and activation of JNK MAPK in cells, and this downstream response to these kinases was used here to test whether the compounds could inhibit TAOK activity in cells (1, 5). COS1 cells were cotransfected with FLAG-tagged JNK and MYC-tagged TAOK1 or TAOK2 and cultures incubated with compound. FLAG-tagged JNK was immunoprecipitated from cell lysates and changes in the phosphorylation and activation of FLAG-JNK determined by immunoblotting samples with the antiactive phospho-JNK-pT183/Y185 antibody. Exogenous TAOK1 or TAOK2 stimulation of JNK phosphorylation was inhibited by compound 43 at $\geq$10 μmol/L and the levels of JNK-pT183/Y185 reduced to those present in control cells transfected with empty vector or kinase-defective TAOK1 (K57A) or TAOK2 (K57A; Fig. 2A and B). These results demonstrate that compound 43 can inhibit TAOK stimulation of JNK phosphorylation in cells. In contrast, compound 63 was unable to prevent the stimulation of JNK phosphorylation by exogenous TAOK1 or TAOK2 in transfected cells, indicating that this small molecule may not be suitable for targeting and inhibiting TAOK activity in cells (Supplementary Fig. S1C). Consequently, all further experiments were carried out using compound 43.

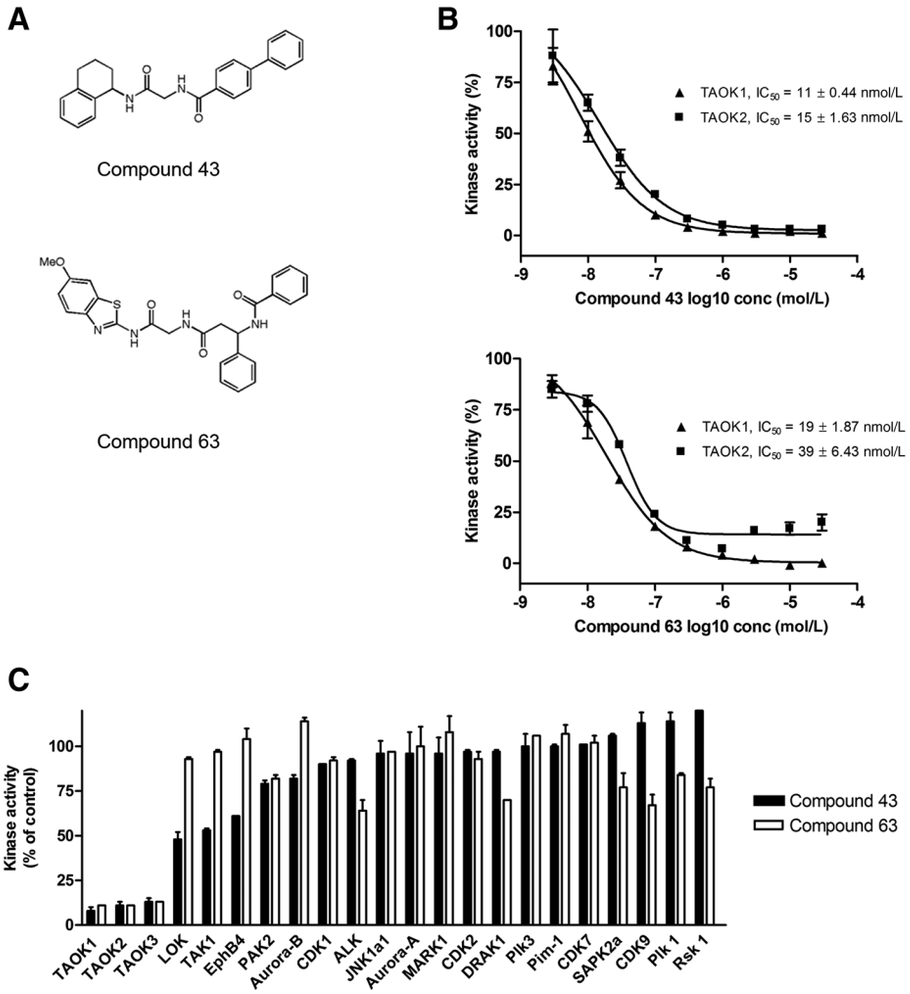

Figure 1.
Small-molecule inhibitors for TAOKs. **A,** Chemical structure of compounds 43 and 63. **B,** Calculated IC_{50} values for compounds 43 and 63 and their inhibition of MBP phosphorylation by TAOKs. **C,** Effects of compound 43 or 63 (0.3 μmol/L) on the catalytic activity of different kinases and phosphorylation of their substrate relative to control samples ($n = 2$).

Q6

TAOKs localize to the cytoplasm and centrosomes during mitosis

Supernumerary centrosomes are a common feature of high-grade and invasive cancers, and a number of breast cancer cell lines were screened to identify appropriate models to represent this aberrant phenotype (27, 28). Cultures were fixed and costained with antibodies to detect pericentrin (centrosomes) and α-tubulin (MTs) plus DAPI (DNA), and significant centrosome amplification (CA, >2) was observed in dividing SKBR3 (38% ± 2% of mitotic cells) and BT549 (31% ± 1.6%) breast cancer cells (Supplementary Fig. S2A). In contrast, nontumorigenic MCF-10A breast cells were predominantly bipolar, and 6% ± 2% of the cell population displayed CA (Supplementary Fig. S2A). Each cell model was also immunostained for phosphorylated and catalytically active TAOK-pS181 (12, 29), which was detected in the cytoplasm and at the centrosomes of mitotic cells but absent in interphase cells (Supplementary Fig. S2B). Noticeably, TAOK-pS181 associated with additional vesicular structures in MCF-10A cells, which are cell type specific but remain to be identified (Supplementary Fig. S2B). TAOK1 and TAOK2 localization in mitotic SKBR3 cells was investigated further by inducing the expression of exogenous GFP-tagged TAOK proteins. TAOK1 and TAOK-pS181 colocalize in the cytoplasm (Fig. 3A), whereas TAOK2 and TAOK-pS181 colocalize with pericentrin at centrosomes (Fig. 3B). TAOK1 and TAOK2 are therefore both catalytically active during mitosis but localize to different cellular sites.

The TAOK inhibitor increases the mitotic population and enhances centrosome and spindle abnormalities in CA cells

The requirement for TAOK activity during mitosis was investigated by treating centrosome-amplified or bipolar cell models with compound 43 and determining changes in cell-cycle distribution using flow cytometry. The percentages of total CA SKBR3 cells in mitosis increased from 1.28% ± 0.22% to 13.54% ± 0.27% after 24 hours of incubation with the TAOK inhibitor and declined thereafter (Fig. 4A, bar chart). The percentages of CA BT549 cells in mitosis also increased from 3.01% ± 0.67% to 9.42% ± 1.0% following treatment with compound 43 for 24 hours (Fig. 4A). In contrast, the percentages of bipolar and nontumorigenic MCF-10A cells in mitosis were 3.82% ± 0.43% when cultures were incubated for 24 hours with compound 43 (Fig. 4A). Analysis of immunostained mitotic cells by confocal microscopy showed that the percentages of mitotic SKBR3 and BT549 cells displaying abnormal centrosomes (>2) or multipolar spindles also increased following treatment with

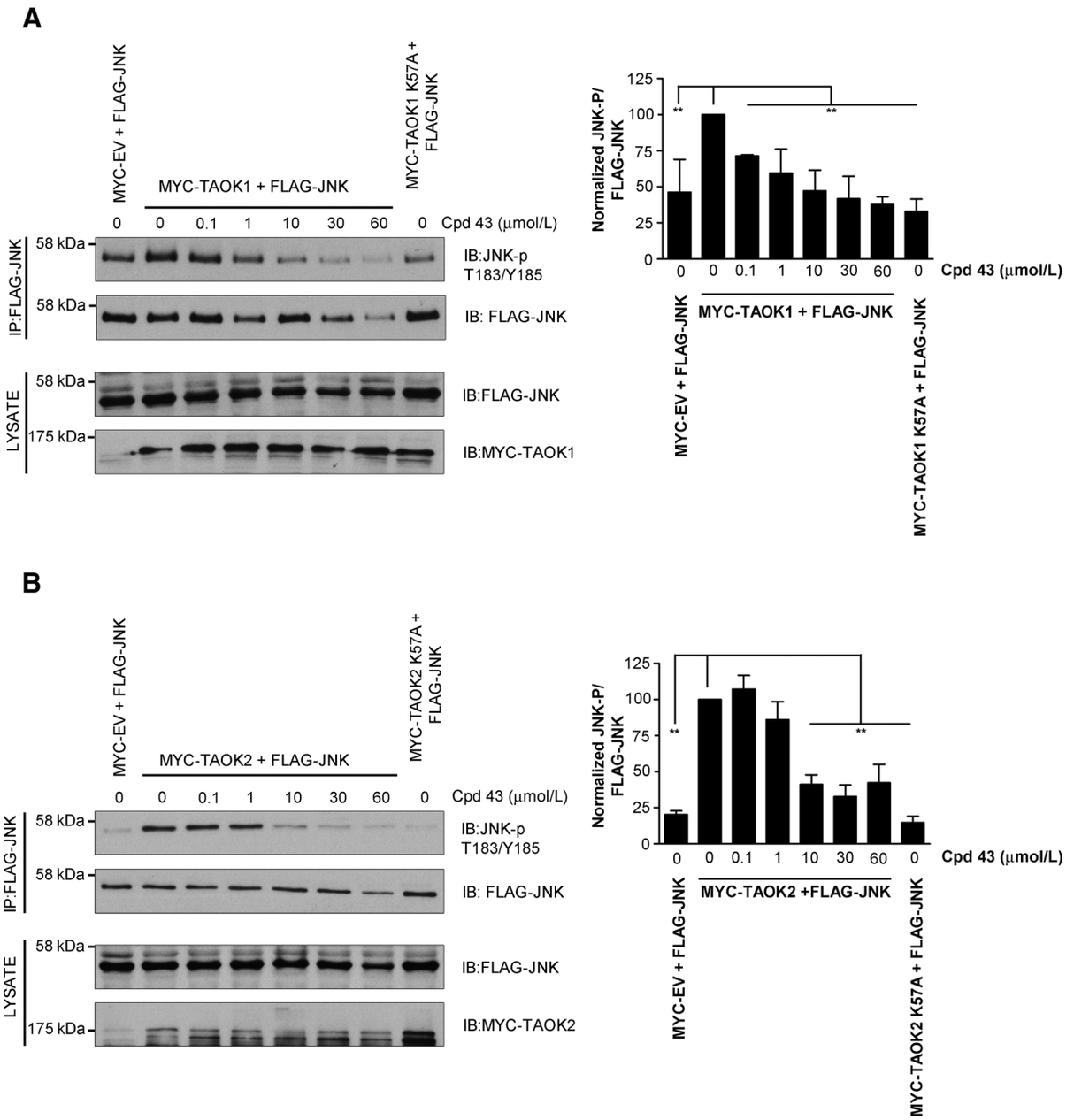

Figure 2.

Compound 43 inhibits phosphorylation and activation of JNK by TAOKs in cells. COS1 cells were cotransfected with FLAG-JNK and either (**A**) pRK5-MYC (MYC-Empty Vector), pRK5-MYC-TAOK1, or pRK5-MYC-TAOK1 (K57A) or (**B**) pRK5-MYC, MYC-TAOK2, or MYC-TAOK2 (K57A), and treated with compound 43 (0–60 μmol/L) as indicated. After 24 hours, FLAG-JNK was immunoprecipitated from cell lysates and bead pellets immunoblotted for FLAG-JNK-pT183/Y185 or total FLAG-JNK. Cell lysates were also immunoblotted for expression of transfected FLAG-JNK, MYC-TAOK1, or MYC-TAOK2. **A** and **B,** Changes in immunoprecipitated FLAG-JNK-pT183/Y185 band intensity relative to total FLAG-JNK (100%) are shown. **, $P < 0.01$; $n = 3$.

compound 43, whereas no significant change in either phenotype was observed when the TAOK inhibitor was added to MCF-10A cells (Fig. 4B and C). Furthermore, siRNA depletion of TAOK1 and TAOK2 expression together but not separately increased the percentages of mitotic SKBR3 or BT549 cells exhibiting abnormal centrosomes (>2), whereas knockdown of either TAOK1 or TAOK2 was sufficient to enhance the occurrence of multipolar spindles (Fig. 4D and E). None of these changes were apparent in mitotic MCF-10A cells with depleted expression of TAOK1 and/or TAOK2 (Fig. 4D and E). Knockdown of TAOK expression was confirmed in all experiments by immunoblotting cell lysates (Supplementary Fig. S3). CA SKBR3 and BT549 breast cancer cells therefore appear more dependent on TAOK activity during mitosis than nontumorigenic and bipolar MCF-10A cells.

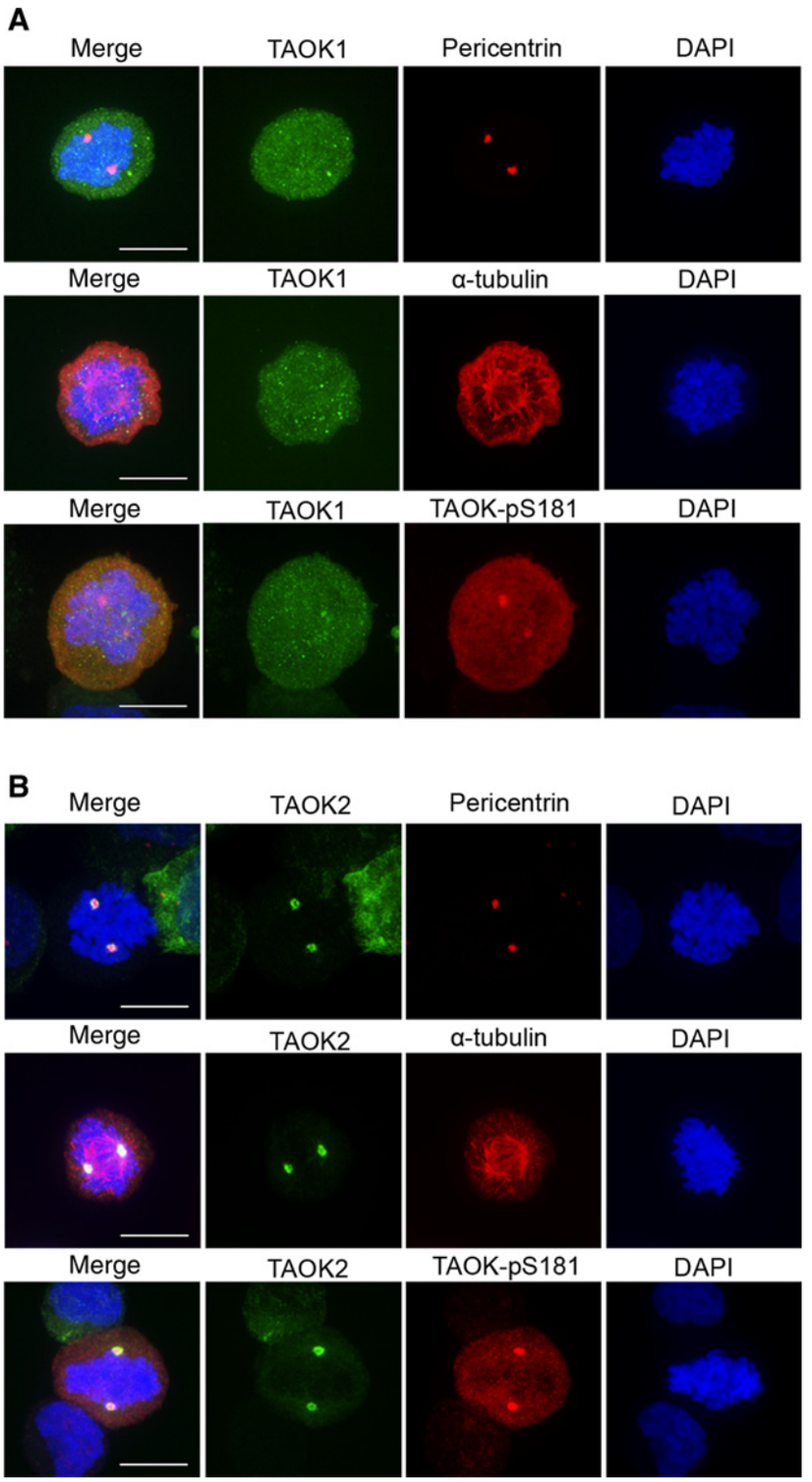

Figure 3.
TAOK1 and TAOK2 localize to the cytoplasm and centrosomes respectively during mitosis. SKBR3 cells expressing (**A**) GFP-TAOK1 or (**B**) GFP-TAOK2 were fixed and costained with antibodies to detect TAOK1, TAOK2, TAOK-pS181, α-tubulin, pericentrin plus DAPI. Representative confocal images are shown. Scale bar, 10 μm.

The TAOK inhibitor prolongs mitosis and promotes cell death in dividing SKBR3 cells

To investigate the effects of the TAOK inhibitor during mitosis, we prepared MCF-10A and SKBR3 cell lines expressing GFP-α-tubulin constitutively and used time-lapse video microscopy. Detailed image analysis showed that SKBR3 cells displayed a mixed mitotic phenotype where 38% ± 1.2% of dividing cells exhibited supernumerary centrosomes and the remaining 62% ± 2% of cells contained two centrosomes and were bipolar. Consequently, bipolar or multipolar SKBR3 cells were scored

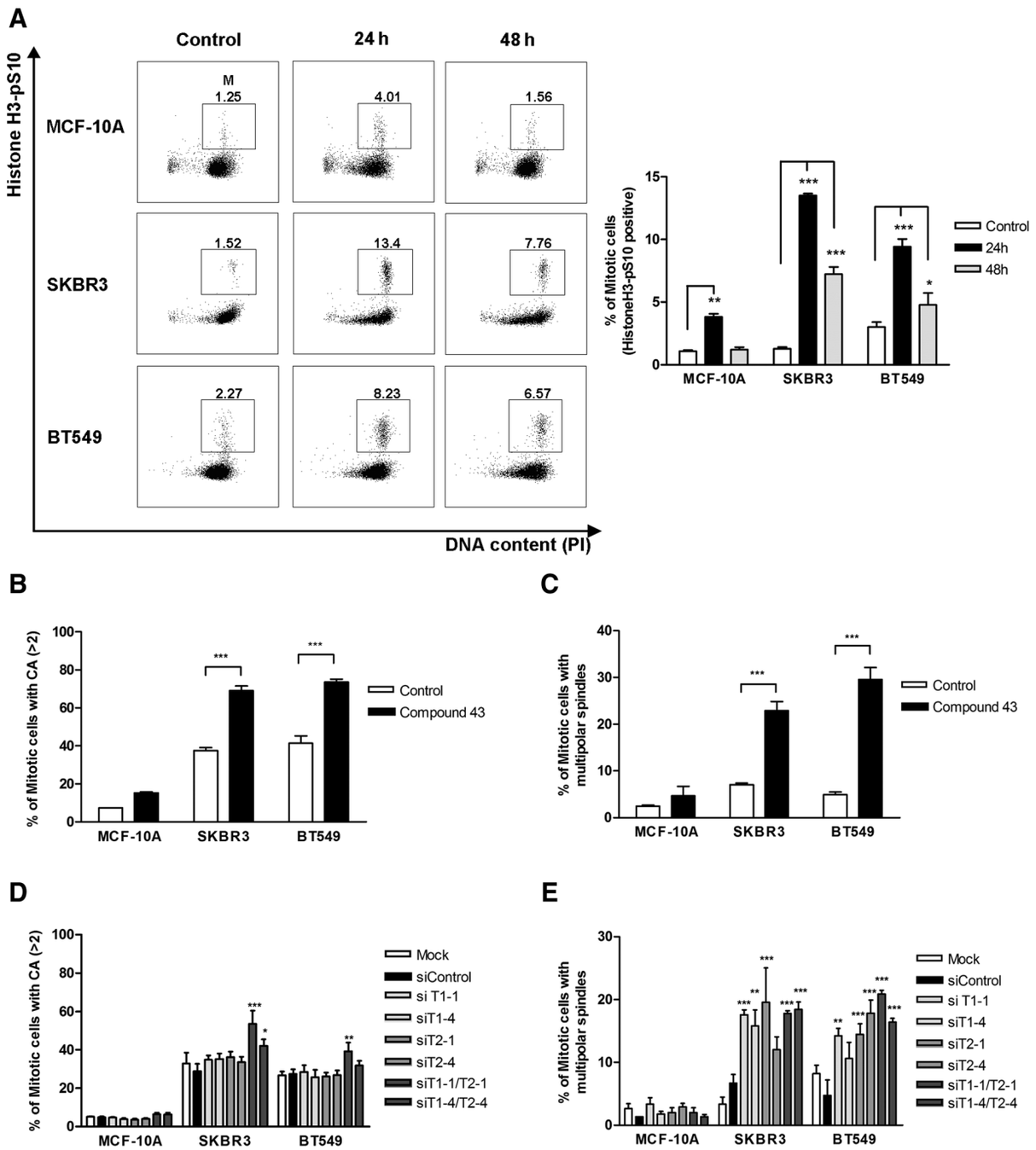

Figure 4.

TAOK inhibition increases the mitotic population and the frequency of CA and multipolarity in dividing SKBR3 and BT549 cells. MCF-10A, SKBR3, and BT549 cells were treated with or without compound 43 (10 μmol/L, 24 or 48 hours, **A–C**) or transfected with siRNA (48 hours, **D** and **E**) as indicated. **A,** Cultures were stained with Alexa-Fluor488-histoneH3-pS10 antibody (mitosis) and PI (DNA). Flow cytometric profiles of cell-cycle distribution are presented in a representative figure and mitotic cells boxed (M). Quantitative analysis of FACS data and changes in % of cells in mitosis are shown. **B** and **C,** Cells were fixed and stained with pericentrin and α-tubulin antibodies plus DAPI and % mitotic cells with >2 centrosomes (**B**) or with multipolar spindles (**C**) determined. **D** and **E,** Cultures were transfected with nontargeting siRNA (siControl) or individual oligonucleotides targeting TAOK1 (siT1-1, siT1-4) or TAOK2 (siT2-1, siT2-4). After 48 hours, cultures were fixed and stained with pericentrin and α-tubulin antibodies plus DAPI and % mitotic cells with >2 centrosomes (**D**) or multipolar spindles (**E**) determined. Note that >150 mitotic cells were analyzed in each experiment. *, $P < 0.05$; **, $P < 0.01$; and ***, $P < 0.001$; $n = 3$.

separately. Each cell culture well was imaged for 48 hours, and the length of time taken between nuclear envelope breakdown and cytokinesis measured for individual cells. Both cell models divide and proliferate under control conditions, although the time taken to complete mitosis was longer in SKBR3 than MCF-10A cells (Fig. 5A). Live cell imaging also showed that MCF-10A cells divide and progress through mitosis in a normal time frame when incubated with or without compound 43 in the culture medium (Fig. 5B and Supplementary Movies S1 and S2 showing representative videos). In contrast, addition of the TAOK inhibitor to SKBR3 cells caused significant increases in the average duration of mitosis in bipolar SKBR3 cells from 89.7 to 465.8 minutes and from 168.3 to 634.3 minutes in multipolar SKBR3 cells (Fig. 5B and Supplementary Movies S3 and S4 showing representative videos). Further analysis of these videos recording the progression of individual SKBR3 cells through mitosis showed that compound 43 caused 19% ± 12% of bipolar cells or 53% ± 14% of multipolar cells to undergo death in mitosis, while the remaining cells exited mitosis and some of these cells are likely to undergo cell death or senescence in the subsequent G_1 phase (Fig. 5C). Notably, the average length of time that MCF-10A cells spend in mitosis did not change significantly in the presence of compound 43 (55 ± 4.4 minutes), and these cells remained viable and continued to proliferate (Fig. 5B and Supplementary Movies S1 and S2).

The TAOK inhibitor induces cell death and inhibits growth of SKBR3 cells

The live imaging results suggest that CA SKBR3 cells are more dependent on TAOK activity for their survival and division than MCF-10A cells. Consequently, the effects of the TAOK inhibitor on MCF-10A and SKBR3 cell viability were investigated next using Annexin V staining and flow cytometry. Treatment with compound 43 caused a significant increase in the percentages of total SKBR3 cells undergoing cell death from 14.8% ± 1.9% (control) to 30.5% ± 5.4% (24 hours) and 42.4% ± 4.9% (48 hours; Fig. 6A, bar chart). In contrast, the percentages of total MCF-10A cells undergoing apoptosis were 13.0% ± 3.4% (control) and increased to 15.1% ± 2.9% (24 hours) and 22.6% ± 3.8% (48 hours) after treatment with the TAOK inhibitor (Fig. 6A). The effect of the TAOK inhibitor on the growth of MCF-10A, SKBR3, and BT549 cells was also investigated. Each cell

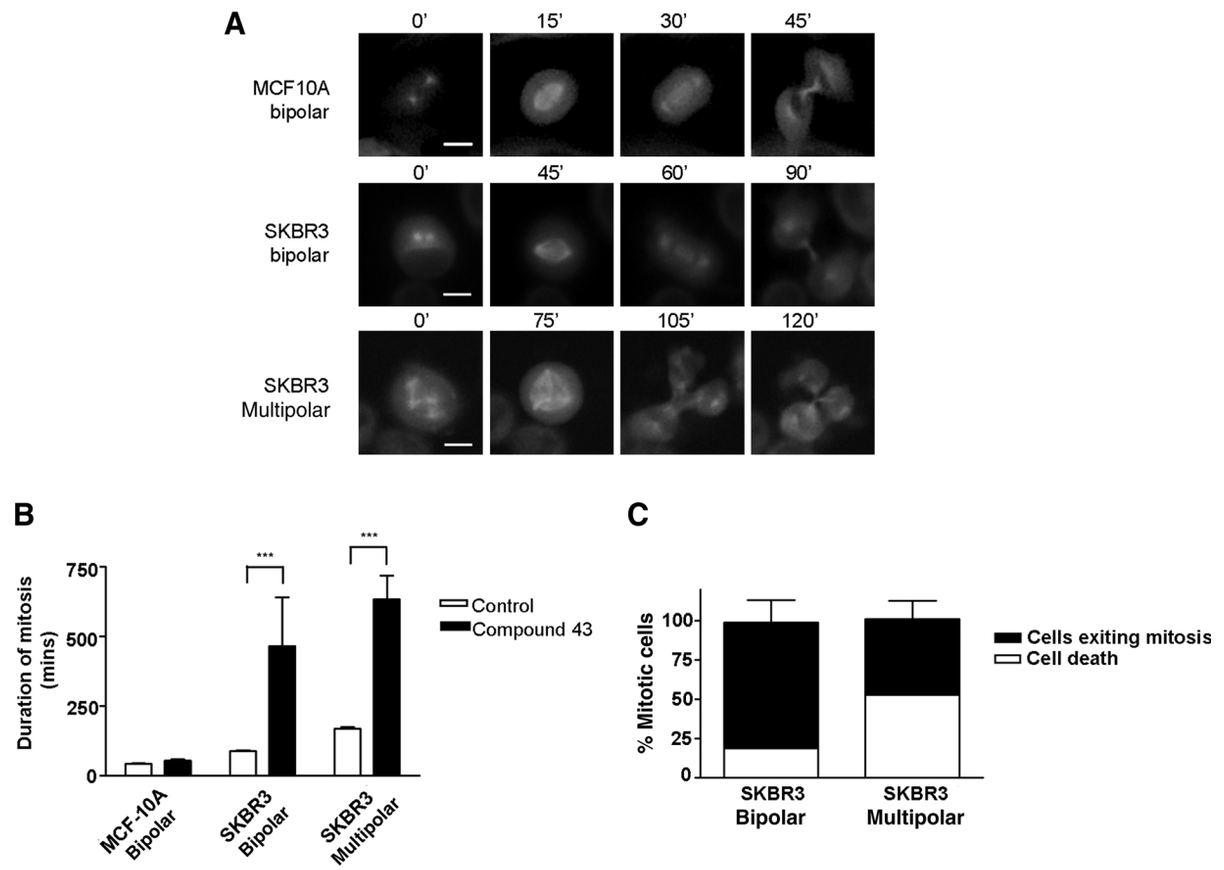

Figure 5.

Compound 43 prolongs mitosis and causes death in dividing SKBR3 cells. MCF-10A or SKBR3 cells expressing fluorescent GFP-α-tubulin were monitored using time-lapse video microscopy and individual mitotic cells analyzed. **A** and **B,** Results showing the time taken for MCF-10A or SKBR3 (bipolar or multipolar) cells to complete mitosis in the absence or presence of compound 43 (5 μmol/L). Scale bar, 10 μm. ***, $P < 0.001$. **C,** The percentages of dividing SKBR3 cells undergoing death in mitosis or exiting mitosis in the presence of compound 43 (48 hours). Note that >120 mitotic cells were analyzed for each condition and per experiment ($n = 3$). Representative time-lapse images are shown in Supplementary Movies S1–S4.

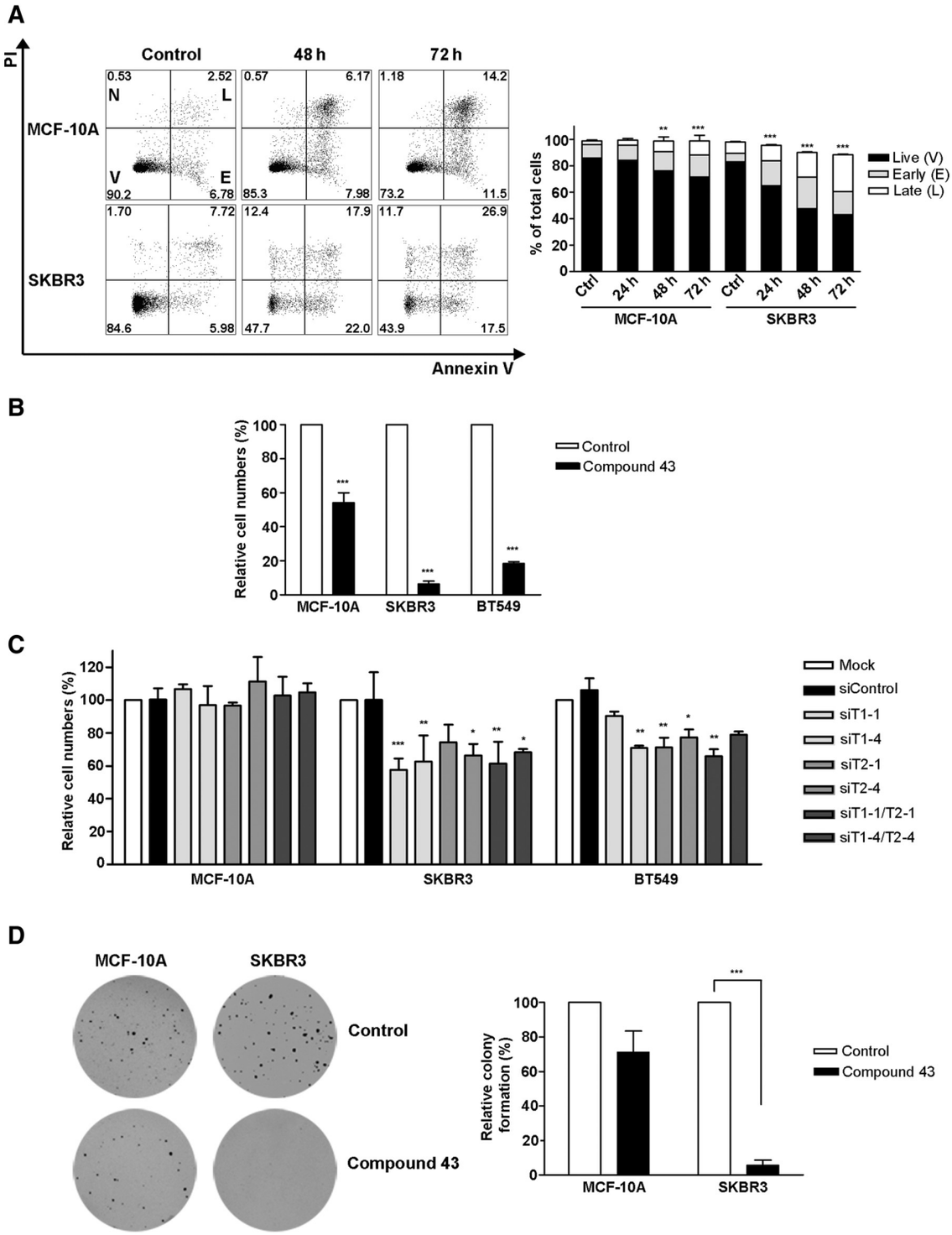

Figure 6.

TAOK inhibition reduces SKBR3 cell viability and growth. **A,** MCF-10A or SKBR3 cells were incubated without (control) or with compound 43, fixed and stained with Alexa-Fluor488–Annexin V (apoptosis) and PI (DNA), and analyzed by FACS to identify live cells (V), early (E), or late (L) apoptotic cells or necrotic (N) cells. A representative figure and quantitative analysis of FACS data are shown. **B,** MCF-10A, SKBR3, or BT549 cells were incubated with compound 43 (10 μmol/L) where indicated and cells detached after 72 hours and counted. **C,** MCF-10A, SKBR3, or BT549 cells were transfected with nontargeting siRNA (siControl) or individual oligonucleotides targeting TAOK1 (siT1-1, siT1-4) or TAOK2 (siT2-1, siT2-4) as indicated and cells detached (72 hours) and counted. **D,** MCF-10A or SKBR3 cells were incubated with or without compound 43 (10 μmol/L) as indicated. After 21 days, colony numbers per plate were determined relative to control cultures (100%). *, $P < 0.05$; **, $P < 0.01$; and ***, $P < 0.001$; $n = 3$.

line was incubated with or without compound 43, and cell numbers determined after 72 hours. Compound 43 reduced SKBR3 and BT549 cell numbers per dish by 94% ± 3% or 82% ± 1.9%, respectively, when compared with untreated control cultures (Fig. 6B). In comparison, MCF-10A cell numbers were reduced by 46% ± 10.3%, when compared with untreated cells (Fig. 6B). SiRNA depletion of either TAOK1 or TAOK2 expression also caused significant reductions in SKBR3 and BT549 cell numbers when compared with control cultures (Fig. 6C), whereas MCF-10A cell numbers were not significantly reduced following depletion of TAOK1 and/or TAOK2, and these cells continued to grow (Fig. 6C and Supplementary Fig. S3). SiRNAs targeting TAOK1 and TAOK2 did not completely abolish protein expression, and this approach was less effective than compound 43 in inhibiting CA cell growth (Supplementary Fig. S3). The effect of compound 43 on soft-agar growth of MCF-10A and SKBR3 cells was also compared over 21 days; the TAOK inhibitor decreased colony numbers by 28% or 94%, respectively (Fig. 6D). Taken together, these results show that CA SKBR3 or BT549 breast cancer cells are more dependent on TAOK activity for their viability and growth when compared with nontumorigenic and bipolar MCF-10A breast cells.

Discussion

Previous reports describing small-molecule inhibitors for TAOKs are limited but have indicated that the protein kinase C inhibitor staurosporine inhibits TAOK2 with an IC_{50} value of 3 μmol/L and the mammalian STE20-like kinase 1 inhibitor 9E1 reduces TAOK2 activity with an IC_{50} value of 0.3 μmol/L (30, 31). However, staurosporine and 9E1 were shown to inhibit many other kinases more potently. A recent high-throughput screen has also identified two compounds, SW034538 and SW083688, that inhibit TAOK2 activity with IC_{50} values of 300 nmol/L and 1.3 μmol/L, respectively; however, further biological characterization of both small molecules is required (32). In this study, we have shown that compounds 43 and 63 act potently to inhibit the activity of TAOK1 and TAOK2 with IC_{50} values of 11 to 15 nmol/L and 19 to 39 nmol/L, respectively, and are ATP-competitive and inhibit the catalytic activity of these kinases preferentially in an assay of 70 kinases. Moreover, activation of JNK MAPK by exogenous cellular TAOK1 or TAOK2 was inhibited by compound 43, demonstrating that this small molecule is an effective inhibitor for TAOKs.

Supernumerary-amplified centrosomes typify high-grade or invasive breast cancer tissues, and appropriate cell models were selected here to represent the aberrant or normal phenotypes (27, 28, 33, 34). Immunostaining experiments showed that TAOKs are phosphorylated and activated specifically during mitosis and that TAOK1 and TAOK2 localized to the cytoplasm or centrosomes, respectively (12). Inhibition or depletion of TAOKs increased the mitotic population and enhanced the occurrence of supernumerary centrosomes and multipolar spindles in dividing CA SKBR3 and BT549 cells. In contrast, bipolar and nontumorigenic MCF-10A cells remained bipolar and continued to proliferate. Live cell imaging of SKBR3 cells treated with compound 43 showed that the duration of mitosis increased and that these cells either failed to exit mitosis and underwent cell death in mitosis or exited mitosis after a significant delay. A subpopulation of SKBR3 cells that undergo bipolar mitosis was also susceptible to the TAOK inhibitor, and a significant proportion of these cells also underwent prolonged mitosis and died. In contrast, MCF-10A cells appeared less dependent on TAOK activity and completed mitosis in the presence of compound 43 in a normal time frame and a bipolar manner, before dividing.

A strong correlation exists between CA and genomic instability in breast cancer, indicating that this abnormal phenotype is likely to contribute to chromosome missegregation and tumorigenesis (28, 34, 35). Supernumerary centrosomes also cause multipolar mitosis and produce nonviable progeny cells owing to lethal gain or loss of chromosomes (17, 36). Malignant and CA cells can however enhance their survival by clustering extra centrosomes to form a pseudo-bipolar spindle, which reduces multipolarity and associated lethal chromosome segregation defects (17, 36, 37). Such cells frequently delay metaphase to allow sufficient MT-kinetochore capture and/or tensions to occur to satisfy the spindle assembly checkpoint, whereas supernumerary centrosomes are also clustered prior to the onset of anaphase (17, 36, 38). In this study and consistent with these previous observations, the duration of mitosis is longer in SKBR3 cells than MCF-10A cells. The TAOK inhibitor prolonged the length of mitosis in SKBR3 cells associated with multipolar mitosis, probably due to centrosome declustering, and enhanced cell death in mitosis. In contrast, MCF-10A cells completed mitosis in a normal time frame and a bipolar manner in the presence of compound 43, and these cells continued to divide and proliferate. SKBR3 cells required TAOK activity for mitotic progression to avoid enhanced multipolarity and associated cell death.

CA can occur due to endoreduplication, cytokinesis failure, cell–cell fusion, PCM fragmentation, or dysregulation of the centrosome cycle (28). However, the mechanisms involved in clustering supernumerary centrosomes are poorly defined. SiRNA screens and live cell imaging studies have implicated functional roles for components of the spindle checkpoint (e.g., Mad2, Bub1, and CENP-E), which are likely activated by incorrect kinetochore-MT attachments and/or tensions, and subsequently delay metaphase to allow centrosome clustering to take place (17, 36, 38). Clustering of centrosomes also requires additional proteins involved in regulating the actin-MT cytoskeleton and spindle positioning (e.g., Myo10A/Myo15 and CLIP190), as well as MAPs and motor proteins, which bundle MTs at the spindle poles (e.g., HSET/KIFC1, Ncd; refs. 38, 39). An additional siRNA screen has identified centrosome clustering roles for E3 ubiquitin ligase APC/C subunits and their cofactors Cdh1 and Cdc20 and their substrates (e.g., Eg5 motor protein), dynein/dynactin and SKA1-3 complexes (40). The screen suggested potential roles for TAOKs, the TAOK binding protein testis-specific kinase (TESK) 1 and LIM domain kinase (LIMK) 2, in the regulation of centrosome clustering (40, 41). TESKs and the related LIMKs can downregulate activity of the actin-severing protein cofilin via phosphorylation, and a mechanism whereby centrosome clustering is inhibited via cofilin-mediated destabilization of cortical actin has been reported (42).

TAOKs can regulate MT dynamics and organization, and their activity is required for mitotic cell rounding and spindle positioning in HeLa cells (7–9, 12). The evaluation of a first-generation TAOK inhibitor here has implicated additional roles for these proteins in regulating the clustering of supernumerary centrosomes to produce a functional pseudo-bipolar spindle in CA breast cancer cells, and a requirement for TAOK activity for such cells to survive and grow. The exact role of TAOK inhibition in centrosome declustering requires further

mechanistic dissection. MT poisons or inhibitors of mitotic kinases such as Aurora and Polo-like kinases or motor proteins (e.g., Eg5) can provide effective cancer therapy; however, such inhibitors are also associated with extreme toxicity and adverse side effects (14, 15, 23–25, 43). Inhibitors of monopolar spindle kinase 1 and the spindle assembly checkpoint have also entered clinical trials, although these compounds appear to exhibit only moderate efficacy as single agents and are more effective when used in combination with drugs such as paclitaxel (44–46). Additional therapeutic strategies are now required to target cancer-specific events, and drugs that stimulate centrosome declustering and multipolarity are likely to kill CA cancer cells selectively, while sparing normal cells (47). The results reported here provide the first indication that TAOKs may provide suitable targets to inhibit and kill CA breast cancer cells selectively. Additional studies are now required for further evaluation of TAOKs as potential drug targets for cancer therapy.

Disclosure of Potential Conflicts of Interest

No potential conflicts of interest were disclosed.

Authors' Contributions

Conception and design: C.-Y. Koo, C. Giacomini, C.M. Marson, S. Linardopoulos, A.N. Tutt, J.D.H. Morris

Development of methodology: C.-Y. Koo, I.A. Tavares, S. Linardopoulos, J.D.H. Morris

Acquisition of data (provided animals, acquired and managed patients, provided facilities, etc.): C.-Y. Koo, M. Reyes-Corral, Y. Olmos, I.A. Tavares, A.N. Tutt, J.D.H. Morris

Analysis and interpretation of data (e.g., statistical analysis, biostatistics, computational analysis): C.-Y. Koo, C. Giacomini, M. Reyes-Corral, Y. Olmos, C.M. Marson, J.D.H. Morris

Writing, review, and/or revision of the manuscript: C.-Y. Koo, C. Giacomini, I. A. Tavares, C.M. Marson, A.N. Tutt, J.D.H. Morris

Administrative, technical, or material support (i.e., reporting or organizing data, constructing databases): C.-Y. Koo, J.D.H. Morris

Study supervision: A.N. Tutt, J.D.H. Morris

Other (redrafting of chemistry content): C.M. Marson

Acknowledgments

We thank Julian Blagg, Daniel Weekes, Nirmesh Patel, Kostas Drosopoulos, Sarah Pinder, Jeremy Carlton, and Ji Ho Rhim for their helpful advice during this study and Laura Price for a donation to support this work.

Grant Support

This study was supported by Breast Cancer Now Project Grant (2012NovPR027) awarded to J.D.H. Morris and A.N. Tutt and Alzheimer's Research UK Project Grant (IRG2014-6) awarded to J.D.H. Morris and D.H. Hanger.

The costs of publication of this article were defrayed in part by the payment of page charges. This article must therefore be hereby marked *advertisement* in accordance with 18 U.S.C. Section 1734 solely to indicate this fact.

Received January 24, 2017; revised May 31, 2017; accepted July 25, 2017; published OnlineFirst xx xx, xxxx.

References

1. Moore TM, Garg R, Johnson C, Coptcoat MJ, Ridley AJ, Morris JD. PSK, a novel STE20-like kinase derived from prostatic carcinoma that activates the c-Jun N-terminal kinase mitogen-activated protein kinase pathway and regulates actin cytoskeletal organization. J Biol Chem 2000;275:4311–22.
2. Hutchison M, Berman KS, Cobb MH. Isolation of TAO1, a protein kinase that activates MEKs in stress-activated protein kinase cascades. J Biol Chem 1998;273:28625–32.
3. Chen Z, Hutchison M, Cobb MH. Isolation of the protein kinase TAO2 and identification of its mitogen-activated protein kinase/extracellular signal-regulated kinase kinase binding domain. J Biol Chem 1999;274:28803–7.
4. Zihni C, Mitsopoulos C, Tavares IA, Baum B, Ridley AJ, Morris JD. Prostate-derived sterile 20-like kinase 1-alpha induces apoptosis. JNK- and caspase-dependent nuclear localization is a requirement for membrane blebbing. J Biol Chem 2007;282:6484–93.
5. Zihni C, Mitsopoulos C, Tavares IA, Ridley AJ, Morris JD. Prostate-derived sterile 20-like kinase 2 (PSK2) regulates apoptotic morphology via C-Jun N-terminal kinase and Rho kinase-1. J Biol Chem 2006;281:7317–23.
6. Tassi E, Biesova Z, Di Fiore PP, Gutkind JS, Wong WT. Human JIK, a novel member of the STE20 kinase family that inhibits JNK and is negatively regulated by epidermal growth factor. J Biol Chem 1999;274:33287–95.
7. Mitsopoulos C, Zihni C, Garg R, Ridley AJ, Morris JD. The prostate-derived sterile 20-like kinase (PSK) regulates microtubule organization and stability. J Biol Chem 2003;278:18085–91.
8. Timm T, Li XY, Biernat J, Jiao J, Mandelkow E, Vandekerckhove J, et al. MARKK, a Ste20-like kinase, activates the polarity-inducing kinase MARK/PAR-1. EMBO J 2003;22:5090–101.
9. Liu T, Rohn JL, Picone R, Kunda P, Baum B. Tao-1 is a negative regulator of microtubule plus-end growth. J Cell Sci 2010;123:2708–16.
10. Timm T, Matenia D, Li XY, Griesshaber B, Mandelkow EM. Signaling from MARK to tau: regulation, cytoskeletal crosstalk, and pathological phosphorylation. Neurodegener Dis 2006;3:207–17.
11. Tavares IA, Touma D, Lynham S, Troakes C, Schober M, Causevic M, et al. Prostate-derived sterile 20-like kinases (PSKs/TAOKs) phosphorylate tau protein and are activated in tangle-bearing neurons in Alzheimer disease. J Biol Chem 2013;288:15418–29.
12. Wojtala RL, Tavares IA, Morton PE, Valderrama F, Thomas NS, Morris JD. Prostate-derived sterile 20-like kinases (PSKs/TAOKs) are activated in mitosis and contribute to mitotic cell rounding and spindle positioning. J Biol Chem 2011;286:30161–70.
13. de Anda FC, Rosario AL, Durak O, Tran T, Graff J, Meletis K, et al. Autism spectrum disorder susceptibility gene TAOK2 affects basal dendrite formation in the neocortex. Nat Neurosci 2012;15:1022–31.
14. Marzo I, Naval J. Antimitotic drugs in cancer chemotherapy: promises and pitfalls. Biochem Pharmacol 2013;86:703–10.
15. Janssen A, Medema RH. Mitosis as an anti-cancer target. Oncogene 2011;30:2799–809.
16. Rieder CL, Maiato H. Stuck in division or passing through: what happens when cells cannot satisfy the spindle assembly checkpoint. Dev Cell 2004;7:637–51.
17. Ganem NJ, Godinho SA, Pellman D. A mechanism linking extra centrosomes to chromosomal instability. Nature 2009;460:278–82.
18. Vitale I, Galluzzi L, Castedo M, Kroemer G. Mitotic catastrophe: a mechanism for avoiding genomic instability. Nat Rev Mol Cell Biol 2011;12:385–92.
19. Castedo M, Perfettini JL, Roumier T, Andreau K, Medema R, Kroemer G. Cell death by mitotic catastrophe: a molecular definition. Oncogene 2004;23:2825–37.
20. Ghersi D, Wilcken N, Simes RJ. A systematic review of taxane-containing regimens for metastatic breast cancer. Br J Cancer 2005;93:293–301.
21. Jordan MA, Wilson L. Microtubules as a target for anticancer drugs. Nat Rev Cancer 2004;4:253–65.
22. Traynor AM, Hewitt M, Liu G, Flaherty KT, Clark J, Freedman SJ, et al. Phase I dose escalation study of MK-0457, a novel Aurora kinase inhibitor, in adult patients with advanced solid tumors. Cancer Chemother Pharmacol 2011;67:305–14.
23. Steeghs N, Eskens FA, Gelderblom H, Verweij J, Nortier JW, Ouwerkerk J, et al. Phase I pharmacokinetic and pharmacodynamic study of the aurora kinase inhibitor danusertib in patients with advanced or metastatic solid tumors. J Clin Oncol 2009;27:5094–101.
24. Hofheinz RD, Al-Batran SE, Hochhaus A, Jager E, Reichardt VL, Fritsch H, et al. An open-label, phase I study of the polo-like kinase-1 inhibitor, BI

2536, in patients with advanced solid tumors. Clin Cancer Res 2010;16:4666–74.
25. Bavetsias V, Linardopoulos S. Aurora kinase inhibitors: current status and outlook. Front Oncol 2015;5:278.
26. Baly DL GA, Ibrahim MA, Jaeger C, Kearney P, Leahy JW, et al. inventor Tao kinase modulators and methods of use. World Intellectual Property Organization International Bureau; 2005.
27. Lingle WL, Barrett SL, Negron VC, D'Assoro AB, Boeneman K, Liu W, et al. Centrosome amplification drives chromosomal instability in breast tumor development. Proc Natl Acad Sci U S A 2002;99:1978–83.
28. Denu RA, Zasadil LM, Kanugh C, Laffin J, Weaver BA, Burkard ME. Centrosome amplification induces high grade features and is prognostic of worse outcomes in breast cancer. BMC Cancer 2016;16:47.
29. Zhou T, Raman M, Gao Y, Earnest S, Chen Z, Machius M, et al. Crystal structure of the TAO2 kinase domain: activation and specificity of a Ste20p MAP3K. Structure 2004;12:1891–900.
30. Zhou TJ, Sun LG, Gao Y, Goldsmith EJ. Crystal structure of the MAP3K TAO2 kinase domain bound by an inhibitor staurosporine. Acta Biochim Biophys Sin (Shanghai) 2006;38:385–92.
31. Anand R, Maksimoska J, Pagano N, Wong EY, Gimotty PA, Diamond SL, et al. Toward the development of a potent and selective organoruthenium mammalian sterile 20 kinase inhibitor. J Med Chem 2009;52:1602–11.
32. Piala AT, Akella R, Potts MB, Dudics-Giagnocavo SA, He H, Wei S, et al. Discovery of novel TAOK2 inhibitor scaffolds from high-throughput screening. Bioorg Med Chem Lett 2016;26:3923–7.
33. Pannu V, Mittal K, Cantuaria G, Reid MD, Li X, Donthamsetty S, et al. Rampant centrosome amplification underlies more aggressive disease course of triple negative breast cancers. Oncotarget 2015;6:10487–97.
34. Lingle WL, Lutz WH, Ingle JN, Maihle NJ, Salisbury JL. Centrosome hypertrophy in human breast tumors: implications for genomic stability and cell polarity. Proc Natl Acad Sci U S A 1998;95:2950–5.
35. Nigg EA. Centrosome aberrations: cause or consequence of cancer progression? Nat Rev Cancer 2002;2:815–25.
36. Godinho SA, Kwon M, Pellman D. Centrosomes and cancer: how cancer cells divide with too many centrosomes. Cancer Metastasis Rev 2009;28:85–98.
37. Quintyne NJ, Reing JE, Hoffelder DR, Gollin SM, Saunders WS. Spindle multipolarity is prevented by centrosomal clustering. Science 2005;307:127–9.
38. Kwon M, Godinho SA, Chandhok NS, Ganem NJ, Azioune A, Thery M, et al. Mechanisms to suppress multipolar divisions in cancer cells with extra centrosomes. Genes Dev 2008;22:2189–203.
39. Chavali PL, Chandrasekaran G, Barr AR, Tatrai P, Taylor C, Papachristou EK, et al. A CEP215-HSET complex links centrosomes with spindle poles and drives centrosome clustering in cancer. Nat Commun 2016;7:11005.
40. Drosopoulos K, Tang C, Chao WC, Linardopoulos S. APC/C is an essential regulator of centrosome clustering. Nat Commun 2014;5:3686.
41. Johne C, Matenia D, Li XY, Timm T, Balusamy K, Mandelkow EM. Spred1 and TESK1–two new interaction partners of the kinase MARKK/TAO1 that link the microtubule and actin cytoskeleton. Mol Biol Cell 2008;19:1391–403.
42. Konotop G, Bausch E, Nagai T, Turchinovich A, Becker N, Benner A, et al. Pharmacological inhibition of centrosome clustering by slingshot-mediated cofilin activation and actin cortex destabilization. Cancer Res 2016;76:6690–700.
43. Infante JR, Kurzrock R, Spratlin J, Burris HA, Eckhardt SG, Li J, et al. A Phase I study to assess the safety, tolerability, and pharmacokinetics of AZD4877, an intravenous Eg5 inhibitor in patients with advanced solid tumors. Cancer Chemother Pharmacol 2012;69:165–72.
44. Wengner AM, Siemeister G, Koppitz M, Schulze V, Kosemund D, Klar U, et al. Novel Mps1 kinase inhibitors with potent antitumor activity. Mol Cancer Ther 2016;15:583–92.
45. Martinez R, Blasina A, Hallin JF, Hu W, Rymer I, Fan J, et al. Mitotic checkpoint kinase Mps1 has a role in normal physiology which impacts clinical utility. PLoS One 2015;10:e0138616.
46. Janssen A, Kops GJ, Medema RH. Elevating the frequency of chromosome mis-segregation as a strategy to kill tumor cells. Proc Natl Acad Sci U S A 2009;106:19108–13.
47. Ogden A, Rida PC, Aneja R. Let's huddle to prevent a muddle: centrosome declustering as an attractive anticancer strategy. Cell Death Differ 2012;19:1255–67.

AUTHOR QUERIES

AUTHOR PLEASE ANSWER ALL QUERIES

Q1: Page: 1: AU: Per journal style, genes, alleles, loci, and oncogenes are italicized; proteins are roman. Please check throughout to see that the words are styled correctly. AACR journals have developed explicit instructions about reporting results from experiments involving the use of animal models as well as the use of approved gene and protein nomenclature at their first mention in the manuscript. Please review the instructions at http://aacrjournals.org/content/authors/editorial-policies#genenomen to ensure that your article is in compliance. If your article is not in compliance, please make the appropriate changes in your proof.

Q2: Page: 1: Author: Please verify the drug names and their dosages used in the article.

Q3: Page: 1: Author: Please verify the affiliations and their corresponding author links.

Q4: Page: 1: Author: Please verify the corresponding author details.

Q5: Page: 1: Author: Units of measurement have been changed here and elsewhere in the text from "M" to "mol/L," and related units, such as "mmol/L" and "μmol/L," in figures, legends, and tables in accordance with journal style, derived from the Council of Science Editors Manual for Authors, Editors, and Publishers and the Système international d'unités. Please note if these changes are not acceptable or appropriate in this instance.

Q6: Page: 4: Author: Please confirm quality/labeling of all images included within this article. Thank you.

Q7: Page: 11: AU:/PE: The conflict-of-interest disclosure statement that appears in the proof incorporates the information from forms completed and signed off on by each individual author. No factual changes can be made to disclosure information at the proof stage. However, typographical errors or misspelling of author names should be noted on the proof and will be corrected before publication. Please note if any such errors need to be corrected. Is the disclosure statement correct?

Q8: Page: 11: Author: The contribution(s) of each author are listed in the proof under the heading "Authors' Contributions." These contributions are derived from forms completed and signed off on by each individual author. As the corresponding author, you are permitted to make changes to your own contributions. However, because all authors submit their contributions individually, you are not permitted to make changes in the contributions listed for any other authors. If you feel strongly that an error is being made, then you may ask the author or authors in question to contact us about making the changes. Please note, however, that the manuscript would be held from further processing until this issue is resolved.

Q9: Page: 11: Author: Please verify the headings "Acknowledgments" and "Grant Support" and their content for correctness.

Q10: Page: 12: Author: Please verify the title in ref. 26 for correctness and also provide publisher location.

AU: Below is a summary of the name segmentation for the authors according to our records. The First Name and the Surname data will be provided to PubMed when the article is indexed for searching. Please check each name carefully and verify that the First Name and Surname are correct. If a name is not segmented correctly, please write the correct First Name and Surname on this page and return it with your proofs. If no changes are made to this list, we will assume that the names are segmented correctly, and the names will be indexed as is by PubMed and other indexing services.

First Name	**Surname**
Chuay-Yeng	Koo
Caterina	Giacomini
Marta	Reyes-Corral
Yolanda	Olmos
Ignatius A.	Tavares
Charles M.	Marson
Spiros	Linardopoulos
Andrew N.	Tutt
Jonathan D.H.	Morris